Exploring the boundaries of Solar Home Systems (SHS) for off-grid electrification: Optimal SHS sizing for the multi-tier framework for household electricity access

Nishant Narayan[a,*], Ali Chamseddine[a], Victor Vega-Garita[a], Zian Qin[a], Jelena Popovic-Gerber[b], Pavol Bauer[a], Miroslav Zeman[a]

[a] Department of Electrical Sustainable Energy, Delft University of Technology, Delft, the Netherlands
[b] Klimop Energy, the Netherlands

HIGHLIGHTS

- Optimal sizing methodology for solar home system (SHS) taking into account battery lifetime.
- Genetic algorithm-based multi-objective optimization approach.
- Optimal SHS sizing for each tier of the multi-tier framework (MTF) for household electricity access.
- Limits of standalone SHS for electrification identified for higher tiers of MTF.

ARTICLE INFO

ABSTRACT

With almost 1.1 billion people lacking access to electricity, solar-based off-grid products like Solar Home Systems (SHS) have become a promising solution to provide basic electricity needs in un(der)-electrified regions. Therefore, optimal system sizing is a vital task as both oversizing and undersizing a system can be detrimental to system cost and power availability, respectively. This paper presents an optimal SHS sizing methodology that minimizes the loss of load probability (LLP), excess energy dump, and battery size while maximizing the battery lifetime. A genetic algorithm-based multi-objective optimization approach is utilized to evaluate the optimal SHS sizes. The potential for SHS to cater to every tier of the Multi-tier framework (MTF) for measuring household electricity access is examined. The optimal system sizes for standalone SHS are found for different LLP thresholds. Results show that beyond tier 2, the present day SHS sizing needs to be expanded significantly to meet the load demand. Additionally, it is deemed untenable to meet the electricity needs of the higher tiers of MTF purely through standalone SHS without compromising one or more of the system metrics. A way forward is proposed to take the SHS concept all the way up the energy ladder such that load demand can also be satisfied at tier 4 and 5 levels.

1. Introduction

Almost 1.1 billion people lacked access to electricity in 2016 [1]. Most of these regions fortunately fall in latitudes that receive abundant sunshine. Additionally, as grid extension is not an immediate solution in most of the unelectrified regions, solar-based products like Solar Home Systems (SHS) have become an important stopgap solution.

An SHS is usually defined as a solar PhotoVoltaic (PV) generator rated 11–20 Wp (for entry level SHS) to more than 100 Wp (high power SHS) and a suitable battery storage [2]. The term Solar Home Systems may be used interchangeably with a standalone PV system, although the term has largely come to be used in the context of off-grid electrification.

1.1. Multi-tier framework (MTF) for household electricity access

Traditional view of looking at the electricity access as have/have-not condition is severely restricting. In reality, having access to a certain level of electricity (for example lights and mobile phone charging) leads to improved living conditions, thereby necessitating higher

---

Table 1
Multi-tier matrix for measuring access to household electricity supply. Sourced from [4].

	Tier 1	Tier 2	Tier 3	Tier 4	Tier 5
Energy and peak power rating	> 12 Wh & > 3 W	> 200 Wh & > 50 W	> 1 kWh & > 200 W	> 3.4 kWh & > 800 W	> 8.2 kWh & > 2 kW
Availability (hrs/day)	> 4	> 4	> 8	> 16	> 23
Availability (hrs/evening)	> 1	> 2	> 3	> 4	> 4
Reliability	–	–	–	< 14 disruptions per week	< 3 disruptions per week
Quality	–	—	–	Voltage problems do not affect the use of desired appliances	
Affordability	–	–	–	Cost of 365 kWh/year < 5% of household income	
Legality	–	–	–	Bill is paid to the utility or authorized representative	
Health & Safety	–	–	–	Absence of past accidents and high risk perception in the future	

electricity needs in the future [3]. To capture the multi-dimensional nature of electricity access, a multi-tier framework (MTF) was proposed by [4]. Table 1 captures the MTF as described in [4]. Climbing up the so-called electrification ladder can therefore also be viewed in terms of moving up the tiers within the MTF. Although the notion of MTF is independent of the type of energy source that enables electrification, in this study, we consider solar PV being the only energy source and battery being the energy storage. In this paper, an optimal sizing methodology is introduced to optimally size SHS for every tier of the MTF, which gives insights on the level of PV and battery storage needed to enable electrification across the various tiers.

1.2. Importance of optimal SHS sizing

SHS sizing comprises the PV sizing, battery sizing, and the sizing of the power converters. PV sizing mainly depends on the total energy needed from the PV generator, which in turn depends on the load profile. A lower than adequate PV size results in system failure or a high number of loss of load events, i.e., high loss of load probability (LLP). LLP is a system metric that quantifies the system's reliability in meeting the load demand, as explained in detail in Section 2.1. A higher than adequate PV size, however, increases the amount of energy dumped — when the load is satisfied and the battery is full.

Power converter sizing mainly depends on the peak power of the PV and the load. Some degree of dimensioning flexibility can be achieved depending on the undersizing of the converter. A lower than peak power of the converter may not be suited for peak power operation but can perform more efficiently at most of the other operating points. This depends mainly on the frequency of occurrence of the different power levels expected throughout the operation of the converter. Thus, a suitably lower than peak sized converter can lead to cost savings. Compared to PV and power converter, however, battery sizing is far more involved.

The battery is a vital component of the SHS that not only enables energy storage of the PV output but also caters to the load when there is no solar generation. However, the battery is the most expensive SHS component while suffering from low lifetimes as compared to other SHS components. Additionally, a smaller than adequate battery size will result in failure to meet the load requirements (high LLP), while an oversized battery will drastically increase the upfront costs of the system. Also, a larger battery size can lead to lower Depth of discharge (DOD) levels, and therefore higher lifetime, whereas a smaller battery size can lead to lower lifetimes due to the deep DOD levels [5,6]. Usual battery lifetimes are much lower than typical PV module lifetime of 25 years. Therefore, a higher battery lifetime is advantageous as it means fewer replacements during the SHS lifetime. Battery costs and lifetime thus have an intricate relationship, making battery sizing extremely relevant albeit challenging in SHS design. Battery sizing and lifetime can, therefore, be considered as critical parameters when dimensioning an SHS.

An optimal SHS size can thus be considered as one that results from an SHS dimensioning exercise that minimizes the LLP, energy dump, and battery size while maximizing the battery lifetime.

1.3. Literature study

In general terms, most sizing-based studies utilize sizing criteria that result in a good trade-off between the system reliability (or power availability) and system investment cost. Previous studies have dealt with the sizing problem by only looking at one or two metrics, including LLP [7,8], system cost, and battery lifetime [9]. LLP has been considered as an objective in [10] as well as a constraint. In [11], the main objective function was to minimize the total SHS investment cost, while keeping LLP ⩽ 2%. LLP was also used as the primary sizing criterion for an off-grid PV-battery system in Bolivia [12], where the system size was determined for three different case studies: a household, school, and health center.

Additionally, battery lifetime has been included as a key parameter in a single weighted objective optimization for a PV array, diesel generator and battery system to minimize battery degradation and fuel consumption [13]. Similarly, the optimal sizing of a PV-battery-diesel generator hybrid system has been investigated [14], paying special attention to system cost and environmental impact of the off-grid system. In this case, the levelized cost of electricity and the carbon footprint of energy are defined as the main metrics that must be minimized.

Other sizing methods are based on intuitive "rules of thumb". The concept of days of autonomy (DOA) for battery sizing, which consists of finding the storage size that can fulfill the load for a predefined amount of days in the absence of solar generation is an example [15]. Another example is the concept of nights of autonomy (NOA). Both the DOA and NOA concepts are discussed in Section 2.2. More complex optimization methods have been introduced over the past years, especially iterative optimization approaches where the system performance for the objective is iteratively evaluated across the decision variable space [16,17]. For instance, a standalone PV-battery system has been dimensioned based on loss of power probability and life cycle cost using an iterative procedure [18].

However, the main drawback of these techniques is that the system is only optimized based on one objective function. Therefore, a system with multiple trade-offs, or objective functions, has not been completely tackled, especially for the application of solar home systems. In comparison, multi-objective optimization (MOO) techniques offer better applicability. Nowadays, MOO techniques based on artificial intelligence are widely used, which are generally more robust, and are better equipped to deal with multi-objective optimization problems [19]. Among them, Genetic Algorithms (GA) are powerful meta-heuristic techniques that are capable of reaching global optima with high accuracy and appropriate computational speed [20]. Former studies using MOO techniques in PV systems show different focus areas compared to our study. In [21], authors quantify the trade-offs between economic and environmental performances of rural solar PV projects. Authors in [22] use a sizing algorithm based on Particle Swarm Optimization (PSO) for a PV-battery-hydrogen fuel cell-based hybrid system. There is a clear research gap in literature with respect to studies focusing on optimal sizing of present-day SHS, especially taking into account battery lifetime as one of the objectives.

In this study, the different SHS parameters need to be optimized simultaneously, making the MOO a necessity. Consequently, in this study, we use a GA algorithm for the task of optimal sizing of an SHS for different electrification levels defined by the MTF. In this optimization, the PV rating, battery capacity, and converter sizes are obtained taking into account the most optimum combination of LLP, excess energy, battery size, and battery lifetime.

1.4. Contributions of this paper

Following are the main contributions of this paper.

1. An optimal sizing methodology for SHS is presented that minimizes the LLP, excess energy, and battery size while maximizing the battery lifetime specific to SHS applications.
2. For the first time, optimal SHS sizing is investigated for the various tiers of MTF for household electricity access.
3. Inadequacies of standalone SHS are highlighted for higher tiers of electrification and a possible alternative is proposed for climbing the so-called electrification ladder.

2. System metrics and parameters

2.1. System metrics

The system metrics used in this work are discussed below.

2.1.1. Loss of Load Probability

The Loss of Load probability is a measure of the system downtime. It is defined as the ratio of the amount of time the system fails to deliver the demanded power to the total amount of operation time the system was designed to deliver power for [8]. For modelling and simulating off-grid systems, this is an application specific or a user-defined constraint. For e.g., in [8], the LLP over a year was constrained to 1.8%, and in [23], a similar metric had a minimum limit of 2%.

$$LLP = \frac{\sum_{i=1}^{N} t_{\text{downtime},i}}{N}$$
(1)

where $t_{\text{downtime},i}$ takes a value of 1 if the system fails to deliver the expected load demand in the ith time interval, and 0 if the system fully meets the load requirement; N is the time period of interest. Since the system is modelled with a 1-min data resolution, $t_{\text{downtime},i}$ is updated every minute, while a 1-year long period of interest yields an N value of 525600.

The choice of LLP can also be dependent on the application. For instance, [15] states that the recommended LLP values for domestic illumination, appliances, and telecommunications applications are 0.01, 0.1, and 0.0001 respectively.

2.1.2. Unsatisfied load energy (E_{fail})

E_{fail} quantifies the unmet energy demand in kWh over a given period of time. In this study, it is mathematically defined as the summation of the unsatisfied energy over a year for each time interval i, as shown in Eq. (2).

$$E_{\text{fail}} = \sum_{i=1}^{N} E_{\text{unsatisfied},i}$$
(2)

2.1.3. Energy dump (E_{dump}) and dump ratio (R_{dump})

This is the total amount of energy that is unused when the local battery is full and the load demand is met while the PV can still generate more power. In this study, this value is considered over a period of 1 year for the system. In order to make relative comparisons easier, a term dump ratio is introduced, which is the ratio between the total energy dump of the system in a year divided by the annual load energy

need, as seen in Eq. (3).

$$R_{\text{dump}} = \frac{E_{\text{dump}}}{E_{\text{load,year}}}$$
(3)

2.1.4. SHS size

SHS size corresponds to the electrical dimensions of PV, battery and the power converters. Typically, this is specific to the rated power of the PV in Wp, total battery capacity in Wh, and peak power rating in W of the converter.

2.1.5. Battery lifetime

This is the lifetime in years of operation after which the battery capacity reduces to below 80% of its nominal rated capacity. At the end of this period, the battery is said to have reached its end of life (EOL).

2.2. System parameters

The following are the other important system parameters that are referred to in this paper.

2.2.1. State of charge and depth of discharge

The state of charge (SOC) refers to the battery charge as a fraction of the nominal capacity, while the depth of discharge (DOD) refers to the capacity discharged as a fraction of the initial capacity [5].

2.2.2. State of health

State of Health (SOH) is indicative of the fraction of the nominal rated battery capacity actually available for cycling.

2.2.3. Days of autonomy (DOA)

Days of autonomy refers to the number of days a particular battery size is capable of powering the full load demand assuming there is no PV generation. This is often used in approximate battery sizing. For e.g., a battery size in Wh can potentially be written as shown in Eq. (4).

$$E_{\text{batt}} = \frac{E_{\text{load}} \cdot n_{\text{DOA}}}{\overline{DOD} \cdot \eta_{\text{batt}}}$$
(4)

where E_{load} is the load energy requirement over a day, n_{DOA} is the number of days of autonomy, η_{batt} is the average battery efficiency, and $\overline{DOD}$ is the average DOD of the intended battery cycling. Practitioners often use DOA or NOA to size the battery as a "rule of thumb". However, this can lead to inaccurate and suboptimal system sizing, as shown later in Section 4.1.

2.2.4. Nights of autonomy (NOA)

Nights of autonomy refers to the number of nights (night = non-sunlight hours of the day) where a battery can completely power the load demand assuming no PV generation to recharge the battery. This is also used in approximate battery sizing. For e.g., a battery size in Wh can potentially be written as shown in Eq. (5).

$$E_{\text{batt}} = \frac{E_{\text{nightload}} \cdot n_{\text{NOA}}}{\overline{DOD} \cdot \eta_{\text{batt}}}$$
(5)

where $E_{\text{nightload}}$ is the load energy requirement in the non-sunlight hours in a day, and n_{NOA} is the number of nights of autonomy.

3. Methodology

The various steps employed in the methodology of this study are described in this section. Section 3.1 presents the inputs to the SHS model, Section 3.2 presents the architecture of the system, Section 3.3 describes a dynamic PV output modeling method, Section 3.4 describes the steps involved in battery lifetime modelling, Section 3.5 discusses the power management scheme used in the standalone SHS, Section 3.6
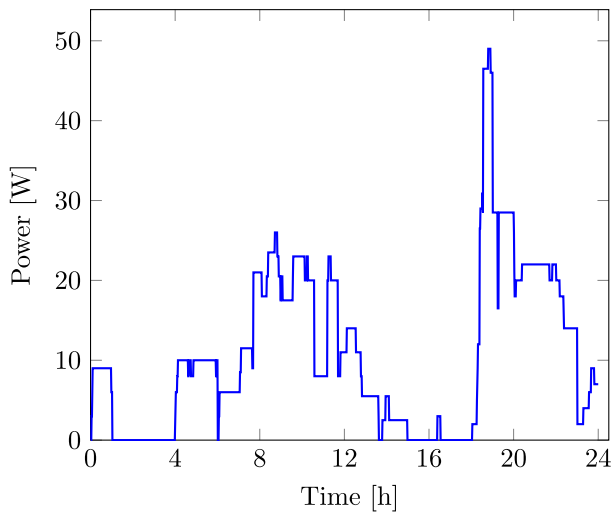
Fig. 1. 1-day load profile of an off-grid household with tier 2 electricity access. The total energy consumption for this day is 257 Wh with a peak of around 49 W. Data sourced from [26].
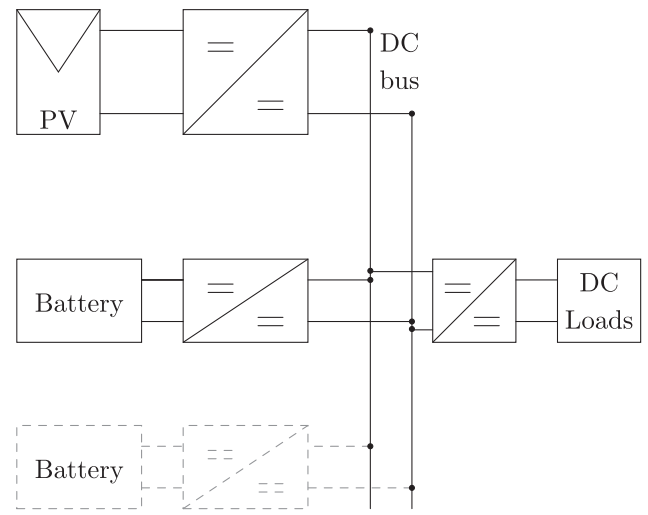

Fig. 2. Modular DC architecture for an SHS that enables intra-household growth option. Dashed battery with converter illustrates the modular capability.

describes the steps used to evaluate the converter rating, and Section 3.7 details a genetic algorithm (GA)-based multi-objective optimization (MOO) approach for SHS sizing.

3.1. Inputs to the SHS model

3.1.1. Location and meteorological inputs to the SHS model

Since the ground level meteorological data was not readily available for the remote rural areas, the data for an Indian city (with 5 Equivalent sun hours of irradiance per day) was taken from the Meteonorm software database [24]. The meteorological data is assumed to be re-presentative of other remote areas in similar latitudes in the tropical regions. The data used in this study has a resolution of 1 min.

The main meteorological inputs used in the SHS model are: (a) Ambient temperature (T_{amb}), (b) Direct Normal Irradiance (G_{DNI}), (c) Diffused Horizontal Irradiance (G_{DHI}), (d) Global Horizontal Irradiance (G_{GHI}), and (e) Wind speed (v_w).

3.1.2. Load profiles for the MTF

Stochastic load profiles were constructed for the various tiers of the MTF in a previous work by the authors [25]. Fig. 1 shows a sample load profile from a representative day for a tier 2 household. The household-level load datasets for all the tiers have been obtained from [25].

Table 2 shows the important load profile characteristics for each tier of the MTF, as obtained in the previous work [25].

3.2. Modular SHS architecture

Climbing up the so-called rural electrification ladder requires expansion of the off-grid system to cater to increased load demand. A modular architecture for SHS is therefore proposed that could potentially allow for expansion of the system at the household level. Fig. 2

shows the modular architecture.

All the SHS components, viz., PV, battery, and DC loads, are connected to the central DC bus via converters. Expansion of the system can be achieved by adding more of the SHS components to the DC bus via a converter, as shown in Fig. 2 with the dashed battery at the bottom. The DC bus can be operated at 12 V, 24 V or 48 V. As more high power loads are connected, a higher bus voltage is recommended to keep the current and therefore cable losses low.

3.3. Dynamic PV output

The dynamic PV output for each minute is calculated based on an elaborate PV model as illustrated in Fig. 3.

There are 4 different kinds of inputs used. Firstly, the location co-ordinates in terms of latitude and longitude are used to determine the sun position throughout the year. The two main parameters that quantify the sun position are the sun Azimuth (E_s) and the sun Altitude (A_s).

Secondly, the ground level irradiance data for the location is used, as mentioned in Section 3.1.1. Along with E_s and A_s, the PV module orientation optimization model uses G_{DNI}, G_{DHI}, and G_{GHI} to evaluate the module azimuth and tilt that maximizes the plane of array irra-diance (G_{POA}). Additionally, the G_{POA} is computed for the optimal azi-muth and tilt.

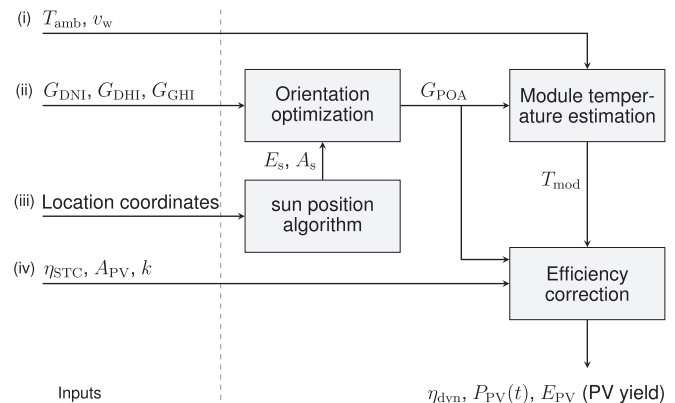The dynamic efficiency (η_{dyn}) of the PV module can be quite

Table 2
Main load profile parameters: maximum peak power P_{max}, minimum peak power P_{min}, and average daily energy $\overline{E_{daily}}$ for each tier based on the 1-year generated load profile [25].

	Tier 1	Tier 2	Tier 3	Tier 4	Tier 5
P_{max} (W)	12	51	154	1670	3081
P_{min} (W)	6	35	113	583	1732
$\overline{E_{daily}}$ (Wh)	50	218	981	3952	9531

Fig. 3. Flowchart explaining the steps involved in calculating the dynamic PV output.

different than its rated efficiency (η_{STC}). As η_{dyn} depends on both the module temperature (T_{mod}) and G_{POA}, the module temperature needs to be estimated. The fluid dynamic model is used to estimate T_{mod} by using T_{amb}, wind speed (v_w), and the calculated G_{POA} as inputs [15].

Finally, the PV efficiency is corrected and the dynamic efficiency η_{dyn} is calculated using the module area (A_{PV}), the temperature coefficient of power for the PV module (k), and η_{STC}. The selected PV module is Jinko Solar JKM265P. Although the rated power is 265 Wp, a normalized dynamic PV output scaled down to 10 Wp is considered for the optimal sizing methodology. The detailed methodology for modelling the dynamic PV output has been described in a previous work done by the authors in [8].

3.4. Estimating battery lifetime

In this study, a valve regulated lead acid (VRLA) battery is considered as the energy storage device. A practical battery lifetime estimation method is considered specific to SHS applications, wherein the battery ageing estimation is based on a dynamic capacity fading model introduced by the authors in [5]. The model uses battery manufacturers' datasheets to refer to the cycle life curves at different temperatures [27]. Constant round-trip efficiency of 90% is considered for the VRLA battery [5].

In the dynamic capacity fading model, micro-cycles of battery activity are considered based on the zero-crossings of the battery current. At the start of the simulation, the battery is assumed to be at 100% SOH. For each micro-cycle, the average DOD ($\overline{DOD_i}$), temperature ($\overline{T_i}$) and total energy throughput (E_{thr}) are evaluated. The proportional number of cycles spent under the same DOD and temperature levels, $\alpha_i(E_{thr_i}, E_{nom})$, is then evaluated, as shown in Eq. (6) [5]. The partial damage incurred by the battery (D_i) in the ith micro-cycle is calculated as shown in Eq. (7) [5].

$$\alpha_i = \frac{E_{thr_i}}{2 \times E_{nom} \times \overline{DOD_i}} \tag{6}$$

$$D_i = \sum_{i=1}^{E} \frac{\alpha_i}{n(\sigma_i)} \tag{7}$$

This damage is then scaled and subtracted from the present SOH, so that when the cumulative damage becomes 1, the SOH reaches 80%. The SOH is therefore dynamically updated as the battery capacity fades with consecutive cycles. When the SOH falls below 80%, the simulation ends. The time at which the simulation ends is the battery lifetime (L) in years.

It should be noted that the lifetime estimation methodology only accounts for the cyclic ageing based on the application usage. Additionally, as the cycle-life curves are taken from the manufacturer's datasheets, choice of a different battery product or type will impact the lifetime calculations.

3.5. Power management scheme for standalone SHS

The algorithm used for power management in every time step (1 min) is shown in Fig. 4. E_{batt} refers to the battery capacity in Wh in any time step.

As shown in the flowchart, at the start of every time step t, the excess power or the load deficit is computed via:

$$P_{excess} = P_{PV} - P_{load} - P_{loss} \tag{8}$$

$$P_{deficit} = P_{load} - (P_{PV} - P_{loss})$$

where P_{loss} is the combined power lost in the PV and load converters. If $P_{excess} > 0$, then the load is fully met, and the excess energy either goes to charge to the battery, or dumped if the battery is full.

The case where $P_{excess} < 0$ means that there is an energy deficit and has to be fed from the battery. If $E_{batt} - E_{batt,min} \geqslant$ the energy deficit for

the time step, then the load is fully met. In the case where the battery cannot feed the load fully or at all, then the unmet load results in E_{fail}. At the instant where $E_{fail} > 0$, LLP = 1 for the given time step. It must be noted that a C-rate limit of 5C was imposed on the battery operation. This process repeats for every time step until the one year simulation is over, corresponding to 1 year of the load data and meteorological data.

3.6. Converter rating

The power converters shown in Fig. 2 need to be appropriately rated. Power rating of each converter is chosen depending on its intended application as seen below.

3.6.1. PV converter sizing

The PV converter optimal size was selected based on the sizing ratio R_S defined in Eq. (9).

$$R_S = \frac{P_{PV,Peak}}{P_{Nom,conv}} \tag{9}$$

where $P_{PV,Peak}$ is the peak PV power and P_{Nom} is the rated converter power.

In the studies conducted in [28,29], the effect of varying R_S on the total yearly energy output from the PV converter was analyzed. The PV array output depends on the geographical location, and rarely has an output that is equal to or larger than its rated peak power. Hence, having $R_S = 1$ or lower for a relatively small time during the year is unnecessary. In this study, the same approach for finding the optimal R_S was performed. The yearly energy yield from the PV module was obtained for values of $0.5 \leqslant R_S \leqslant 1.5$ as shown in Fig. 5.

The figure shows that for $R_S = 0.9$, the maximum energy yield is obtained. However, for $R_S = 1.27$, 96% of the maximum yield is obtained. Hence, for an around 41% reduction in the sizing ratio (from 0.9 to 1.27), only 4% of the energy yield is lost. Therefore, an R_S of 1.27 was selected as the optimal sizing ratio to obtain the PV converter rating $P_{Nom,conv}$, as it is the highest sizing ratio (and therefore most sizing gains) that guarantees more than 95% of maximum achievable yield. Moreover, past studies on solar converter sizing have concluded that a converter could be undersized by up to 30% of the PV array W_p, as undersizing causes an insignificant reduction ($\leqslant 5\%$) in the total yearly energy yield compared to the reduction in its cost [28,29].

3.6.2. Load converter sizing

The load converter was sized according to the peak load for each tier. Hence, for the load converter, $P_{Nom} = P_{max}$, which are the values found in Table 2.

3.6.3. Battery converter sizing

The battery converter is a bidirectional converter that processes power by charging or discharging based on the excess PV generation or greater load demand respectively. Hence, it should be sized appropriately to allow the maximum net charge or discharge power to go in/out of the battery. The P_{Nom} for the battery is then the maximum between the $P_{deficit}$ and P_{excess} values.

3.7. Multi-objective optimization for standalone SHS sizing

Optimal SHS sizing is a complex task that brings to the fore the intricate interplay between the different SHS component sizes and the various system metrics described in Section 2.1. For e.g. a larger battery size can lead in general to longer battery lifetimes (at the cost of increased initial investments), while a smaller battery size will result in loss of load events (high LLP) as there won't be enough stored energy to power the load in the non-sunlight hours. Similarly, a lower than adequate PV size will result in high LLP. However, an indiscriminate increase in PV size will result in high E_{dump} values, which is a waste of
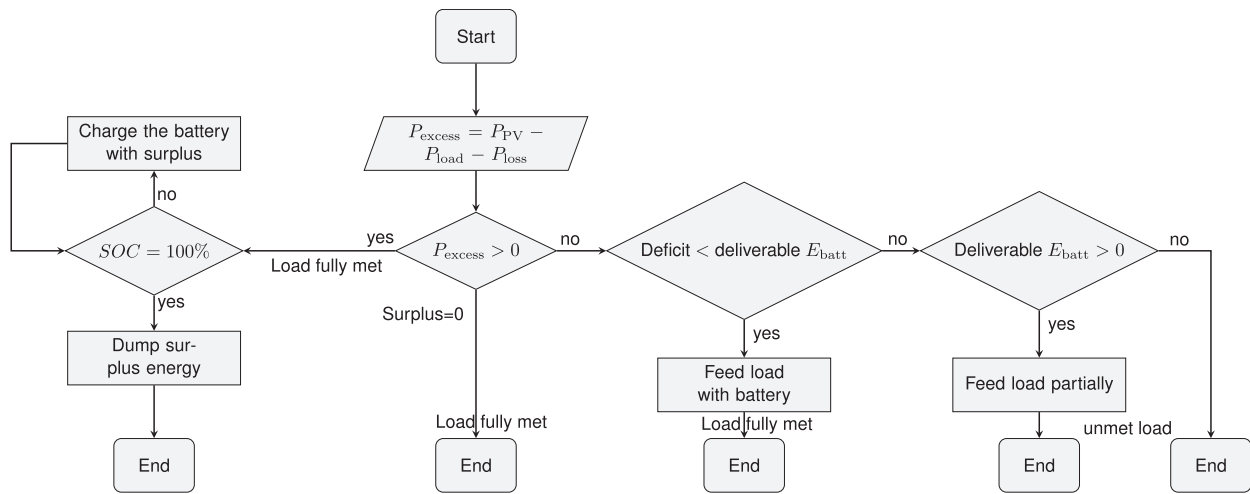
Fig. 4. Flow chart explaining the power management scheme used in the standalone SHS model; it represents the algorithm followed in every time step.
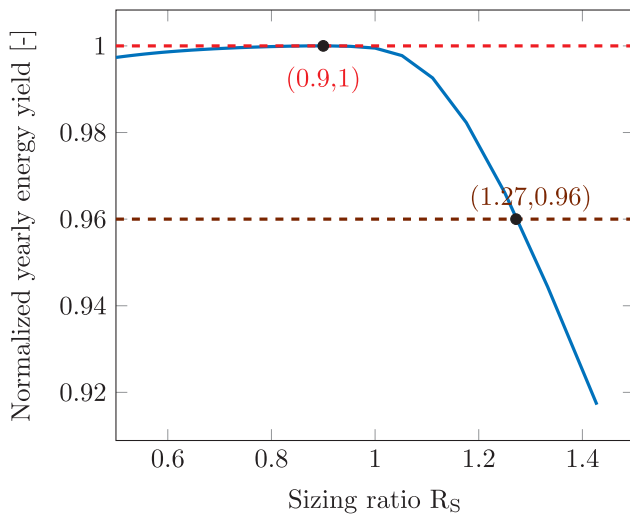

Fig. 5. Normalized energy yield VS R_S.

energy and should be avoided as much as possible. While an increase in PV or battery size increases the initial system costs, a high E_{dump} value increases the levelized cost of kWh of the system.

3.7.1. Decision variables

For the optimal SHS sizing, 3 variables determine the performance of the system based on the various metrics. These are: PV size (Wp), battery size (Wh), and converter ratings (W). However, as seen in Section 3.6, the converter rating is dependent on the PV size and the load. The load profile is a given for the specific SHS application (MTF tier-based usage). Therefore, the primary independent decision variables used in this study are:

(1) the PV size (Wp) and
(2) the battery size (Wh).

3.7.2. Objectives

The main objectives can be written as (a) to minimize total cost (b) to minimize LLP and (c) to minimize E_{dump} (or R_{dump}). However, the total system cost can be considered as a sum total of PV cost, battery cost, and the converter cost. Each of these costs are directly proportional to the rating of the SHS components. Additionally, the battery costs consist of both the initial costs and the replacement costs, owing to the lowest lifetime amongst the other SHS components. As the

replacement costs go down with increasing battery lifetime, minimizing the total battery costs is the same as minimizing the battery size while maximizing the battery lifetime (although battery size and lifetime are not mutually independent variables).

The converter sizes are again dependent on the PV and load and therefore cannot be independently minimized to lower the costs. PV size is in a way already reflected in minimizing the dumped energy (E_{dump}). Therefore, the objective of minimizing total SHS costs can be crystallized down to the objectives of minimizing battery size, maximizing battery lifetime and minimizing E_{dump}. This adaptation of the cost objective into battery size and lifetime helps in avoiding the actual costs in $ or €, for example, and maintains the generality of the methodology and the results.

Consequently, the following objectives are used for multi-objective optimization in this study.

(1) to minimize the battery size
(2) to maximize the battery lifetime
(3) to minimize the LLP and
(4) to minimize the R_{dump}.

3.7.3. Constraints

Constraints are necessary in the MOO process to curtail optimization run times and eliminating unwanted navigation of the algorithm employed within the search space. In this study, constraints were placed on the LLP and the E_{dump}. Although LLP and E_{dump} form part of the objective set, the additional constraints augment the efficiency to the optimization computation. The constraints used in the MOO can be stated as:

(1) LLP $\leqslant 10\%$
(2) $E_{dump} \leqslant$ yearly load or $R_{dump} \leqslant 1$.

3.7.4. Genetic algorithm-based MOO

For performing a multi-objective optimization (MOO), the genetic algorithm toolbox of MATLAB was utilized. The *gamultiobj* function within the GA toolbox of MATLAB is based on a Non-dominated Sorting GA (NSGA)-II variant [30]. Fig. 6 outlines the steps contained in the GA-based MOO used in this study. The functioning of the genetic algorithm can be explained as follows.

1. **Initialization**. The initialization step involves generating a random population of 'N' individuals which represent the first generation. Each individual has a set of characteristics, which are the PV and battery capacity in Wp and Wh, respectively. For example, for an
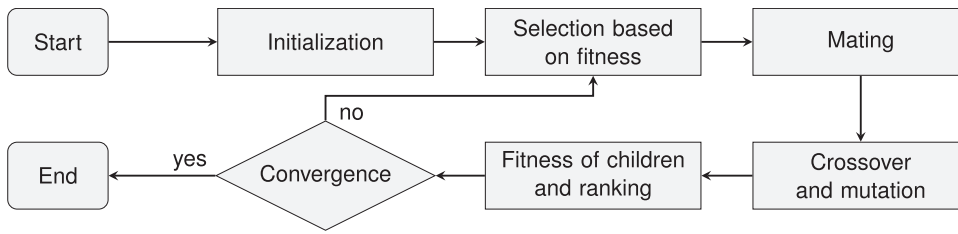
Fig. 6. Flow chart showing the steps followed in the GA-based MOO.

individual X:

$$X = [PV_X, Batt_X] \qquad (10)$$

The final step of initialization also includes evaluating the fitness.

2. **Fitness-based selection**. In this step, the fitness of each individual is assessed according to the objective functions:

$$\text{Obj. functions} = \begin{cases} Min{:}LLP \\ Max{:}L \\ Min{:}E_{\text{dump}} \\ Min{:}E_{\text{batt}} \end{cases}$$

and the fittest individuals are selected for the mating, while the rest are disregarded.

3. **Mating**. A pair from the pool of fittest individuals is selected for mating, producing two offspring individuals that share characteristics from each of the parents. The process is repeated until a new population of 'N' individuals is obtained.

4. **Crossover and mutation**. These two stochastic operators serve to randomly alter the characteristics of some of the "child" population to maintain some variability in the algorithm.

5. **Fitness of children**. The same fitness assessment and selection takes place for the children individuals, which represent the new generation.

6. **Checking convergence criteria** The convergence criteria used are:
   (a) $G_i = G_{\text{max}}$, where G_i is the ith generation
   (b) $\Delta_{S_i} \leqslant \Delta_{S,\text{max}}$ for each objective, where Δ_{S_i} is the spread between the objectives for G_i and G_{i+1}.

If the convergence criteria are met, the optimization process stops. Otherwise, the optimization process repeats from Step 2 until convergence is reached. In Table 3, the parameters and convergence criteria used in this study are shown.

It must be noted that the a multi-objective optimization need not lead to unique optimization solutions. Instead, a Pareto set of solutions is usually obtained, which (in terms of GA) are the individuals with fitness functions that are non-dominated by any other individual in the search space. Here, dominance refers to the attribute of an individual to score lower (better) than all other individuals for that particular fitness function. For e.g., an individual x dominates y in the population when [31]:

$$f_i(x) \leqslant f_i(y) \quad \forall \ i \quad \text{and} \qquad (11)$$

$$f_i(x) < f_i(y) \quad \text{for at least 1 } i$$

Table 3
GA parameters and stopping conditions used in this study.

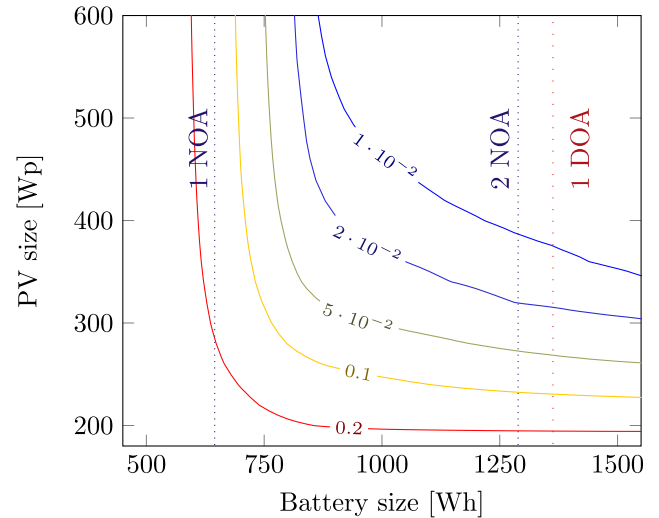| Parameter	Symbol	Value
Population size	N_{max}	25
Generation limit	G_{max}	500
Spread tolerance	$\Delta_{S,\text{max}}$	10^{-4}

Fig. 7. LLP contours based on PV and (VRLA) battery sizes for a tier 3 load profile.

4. Results and discussions

4.1. Dependence of SHS parameters on size

As described in Section 3.7, there is a complex interplay of the various SHS parameters with respect to the SHS size. In this section, the impact of sizing on each of the system metrics (LLP, R_{dump}, and lifetime) is presented.

4.1.1. LLP

Fig. 7 presents a contour plot depicting the variations in LLP depending on the PV and battery size for a tier 3 load profile with VRLA battery. It can be seen that the same LLP can be achieved by either increasing the battery size or the PV size. Moreover, minimal sizing can be achieved if the knee point of the curve is chosen for a given LLP. However, the knee point, or the least distance of the curve from the origin, is a least-cost operating point only if the PV and battery are equally cheap or expensive.

In other words, for the same technology costs ($/Wp and $/Wh), the least-cost operating point is the knee point. Deviations from the knee point to achieve least-cost sizing is possible if the ratio between the technology costs is precisely known. Additionally, also shown in Fig. 7 are the battery sizes based on the days of autonomy and nights of autonomy, represented as vertical lines. It can be seen how a "rule of thumb" of 2 DOA using a "back of the envelope" method to arrive at battery size (refer to Eq. (4)) can result in oversizing of the battery, as even for 1 DOA, Eq. (4) yields a battery size of 1363 Wh for a VRLA battery assuming an 80% DOD. Using NOA method need not be very precise either, and also depends largely on the proportion of the load profile that is in the non-sunlight hours. The exact LLP achieved using such methods will also depend on the operational PV module size. In general, these "rule of thumb"-based approaches can lead to inaccurate battery sizing leading to either an expensive or an inadequately reliable system.
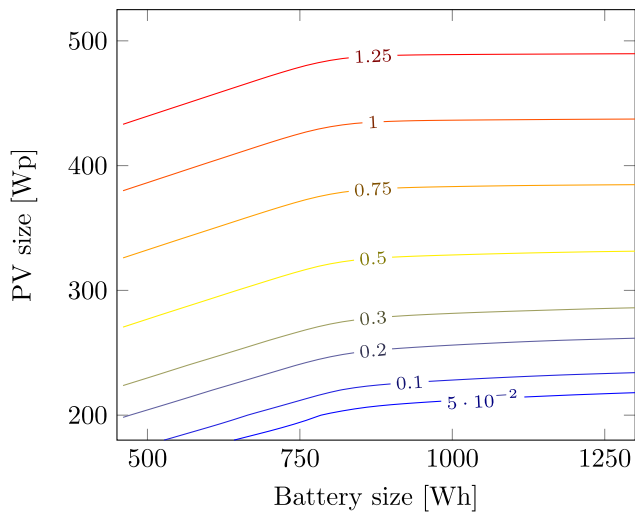
Fig. 8. R_{dump} contours based on PV and (VRLA) battery sizes for a tier 3 load profile.

Fig. 10. LLP VS R_{dump} for a Pareto set of points for the tier 3 case.

4.1.2. Dump ratio

Fig. 8 presents a contour plot depicting the variations in R_{dump} depending on the PV and battery size for a tier 3 load profile with VRLA battery. As seen in the figure, the R_{dump} increases with increasing PV size. To an extent the increase in battery size helps in reducing the dump ratio. However, after around 900 Wh, the increase in battery is almost irrelevant for the considered PV and battery size range. It can already be seen that an interesting trade-off emerges between LLP and R_{dump}. For example, to maintain an LLP of 0.05 and below (Fig. 7), almost 300 Wp of PV module is necessary. On the other hand, a 300 Wp of PV module size will guarantee an R_{dump} of at least 0.3 as seen in Fig. 8.

4.1.3. Battery lifetime

The trade-off between LLP and R_{dump} becomes more intricate when the battery lifetime is considered into the mix. Fig. 9 presents a contour plot depicting the variations in battery lifetime (L) depending on the PV and battery size for a tier 3 load profile with VRLA battery.

For the same PV size, the battery lifetime increases with increasing battery size. For the same battery size, the lowest PV size leads to relatively lowest battery activity and therefore highest lifetime. As the PV size increases for the same battery size, the battery lifetime initially
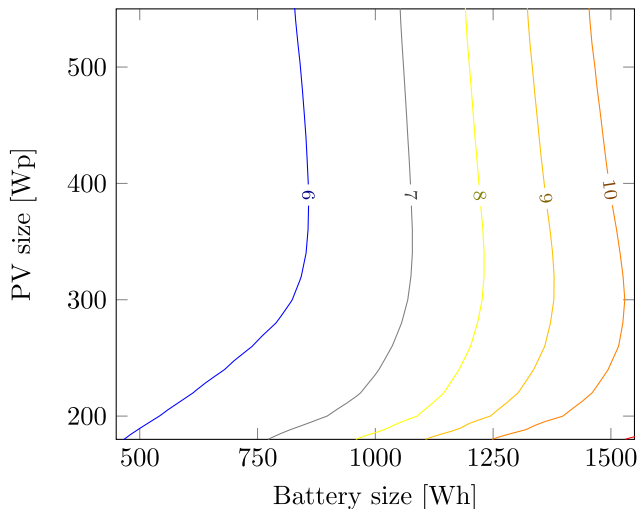
decreases due to increasing battery activity contributing to higher cyclic ageing. However, at the higher end of the PV sizing range, the battery is being operated largely at relatively lower DOD levels, leading to relatively higher lifetimes than the medium PV range.

4.2. Multi-objective optimization for SHS sizing

Based on the methodology described in Section 3.7, a multi-objective optimization was performed for the various objectives. Consequently, different Pareto fronts are obtained that give the optimal PV and battery sizes that dominate at least one objective function without being worse off in the other objectives, as shown in Eq. (11). Fig. 10 shows for the tier 3 case the Pareto set of points for LLP, R_{dump}, which also perform optimally with respect to the other objectives of lifetime and battery size. As expected, the solution space is bounded by the constraints specified in Section 3.7.3.

Figs. 11 and 12 depict the same Pareto set of points for the system metrics of LLP and lifetime, and lifetime and R_{dump}, respectively. Some of the points that were too close to each other have been removed for clarity. It can be seen that the various system sizes represented by the points in the Pareto set perform differently across the various system metrics. As long as the different objectives are not weighted, the applied methodology does not favour a particular system size over another. Therefore, the task of optimal SHS sizing for a particular tier will

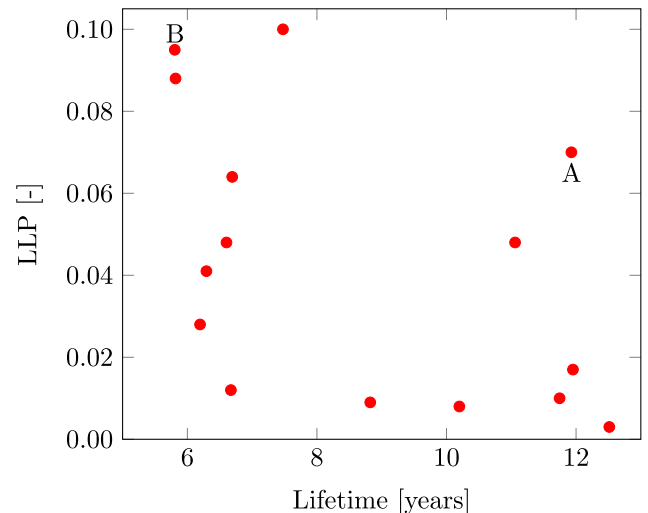Fig. 9. Lifetime contours based on PV and (VRLA) battery sizes for a tier 3 load profile.

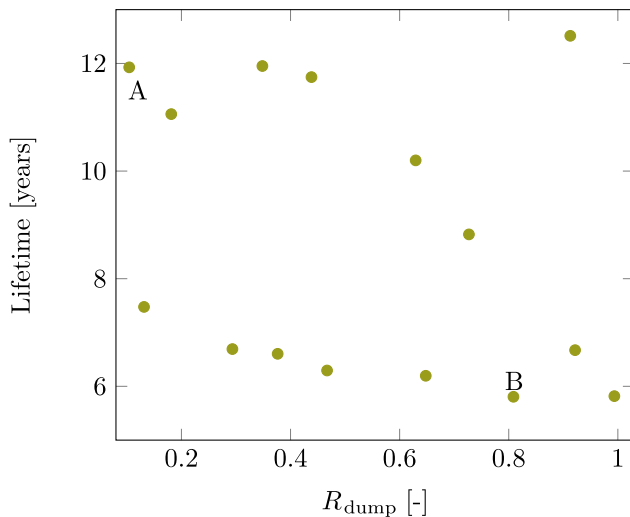Fig. 11. LLP VS lifetime for a Pareto set of points for the tier 3 case.

Fig. 12. Lifetime VS R_{dump} for a Pareto set of points for the tier 3 case.

depend on selecting an optimal size based on additional filters and categorization, as described below in Section 4.2.1.

It should be noted that the GA-based MOO chooses the Pareto front based on the performance across all 4 objective functions and not just the 2 functions described in these figures. Therefore, each figure shows the Pareto points that satisfy not only the two objective functions represented on the x and y-axes, but all four objective functions stated in Section 3.7.2. This is illustrated with the help of 2 labeled Pareto points A and B in Figs. 10–12. Point A satisfies a very high battery lifetime as well as a low R_{dump} (11.93 years and 0.1 respectively), but shows a relatively high LLP (0.07). Furthermore, the battery size, which is also an objective to be minimized in the optimization, is not explicitly represented in the Pareto fronts in Figs. 10–12, but is playing an equally important role in the selection of optimal Pareto points. For example, point A leads to a storage size of 1800 Wh for tier 3 SHS. On the other hand, point B, which seems to be specifically non-dominant for the LLP, Lifetime and R_{dump} simultaneously (0.095, 5.81, and 0.81 respectively), actually has the lowest battery size (720 Wh), and is therefore part of the Pareto front.

4.2.1. Optimal SHS sizes for tiers of the MTF

Similar to the results shown in Figs. 10–12, the MOO was performed for all the tiers of the MTF. To determine the optimal system sizes per tier, a selection has to be made from the Pareto set of points allowing relative trade-offs. Firstly, three different categories of LLP are defined, viz., (a) $LLP \leqslant 0.1$, (b) $LLP \leqslant 0.05$, and (c) $LLP \leqslant 0.02$. Secondly, the smallest battery size that satisfies the above LLP criteria in each category are chosen. This gives rise to unique PV-battery size combinations per tier. Accordingly, the final optimal SHS sizes for every tier of the MTF is shown in Table 4. The table also shows the system metrics for the particular PV and battery size along with the converter sizes.

Based on the methodology followed in Section 3.6, the converter sizes follow the PV rating and load profile. The PV and battery sizes, however, are a direct result of selection of a particular PV-battery combination from the Pareto set. Based on the LLP threshold, the selection of the lowest battery size to meet the LLP criteria gives an interesting mix of system sizes. For instance, as seen in Table 4, the LLP $\leqslant 5\%$ criterion sees lower PV and higher battery sizes as compared to LLP $\leqslant 10\%$ for tiers 3 to 5. This leads to relatively lower R_{dump} values.

4.2.2. The limits of standalone SHS

As seen in Table 4, the PV and battery sizes increase drastically between the tiers, especially when going towards tiers 4 and 5. Additionally, it can be seen that no optimal solutions exist with the given

constraints for tier 5 for $LLP \leqslant 2\%$. This is because larger-sized SHS that could potentially satisfy the LLP criterion would still end up compromising the dump criterion while also leading to extremely high battery sizes. This clearly shows that there is a limit to the level of electricity access a standalone SHS can provide.

For tiers 1 to 3, a small increment in system size (due to climbing up the tiers for e.g.) can be easily achieved, especially in a way such that low LLP values are guaranteed. However, tiers 4 and 5 require significant increase in system sizing, and without the kind of reliability (low LLP) achievable at the lower tiers. Additionally, the presence of high power loads also increases the required converter ratings in tiers 4 and 5. If the LLP threshold is further lowered to $\leqslant 1\%$, even tier 4 has no optimal solution based on the Pareto points. The lowest achievable LLP for tier 4 within the given constraints is 1.5%.

4.2.3. State-of-the-art SHS

It should be noted that the concept of LLP as a vital parameter in system sizing is usually not followed in state-of-the-art SHS. For example, present-day SHS capable of powering up to tier 2 level loads, are sized from 50 Wp, 300 Wh (for an SHS operational in East Africa) to 100 Wp, 1 kWh (for an SHS operational in Cambodia). While this may lead to suboptimal use of the SHS components of PV and battery, having a sizing approach without a reasonable approximation of LLP targets for standalone SHS catering to higher tiers could amplify the suboptimal usage.

Additionally, as most deployed state-of-the-art SHS are rated less than 200 Wp, there is a long way to go if SHS are to enable higher tiers of electrification as ubiquitously as they have been effective with tiers 1 (as pico-solar products) and 2. While tier 3 level electrification still seems to be within reach of state-of-the-art SHS, tier 4 and tier 5 level electrification demand a much bigger expansion from the standalone SHS, which may not be practical to implement when additional aspects like financial viability are considered in off-grid contexts.

4.2.4. Another approach to climbing up the electrification ladder

In the absence of a central grid connection in many of these off-grid regions where SHS are currently deployed, the best way to achieve tier 4 or tier 5 level of electricity access is via a microgrid. However, a centralized islanded microgrid with central PV and storage requires high CAPEX investments, which is also why standalone SHS have seen far greater proliferation than centralized rural microgrids. Moreover, the level of electrification is often a dynamic requirement, as the electricity needs keep increasing with time [3,25]. For e.g., households might not need a direct tier 4 or tier 5 connection, but might move from tier 3 to tier 4 over a span of time. In such a case, it is more practical to envisage a bottom-up SHS-based microgrid borne out of the interconnection of standalone SHS. This would enable the sharing of excess energy between the households while improving the overall system metrics of LLP and R_{dump}. Additionally, individual battery storage requirement might also significantly reduce, along with the converter sizing, depending on the topology of the microgrid. This would especially help in alleviating the demanding system sizes at tiers 4 and 5.

4.3. Recommendations and future work

The set up of such an interconnected system is a complex research topic in itself and future work is recommended on it to examine the impact on the overall system metrics of the microgrid as compared to standalone SHS. An interconnected SHS-based microgrid model must be built to further explore the concept of climbing up the energy ladder (higher tiers of the MTF). The gains in terms of system sizing in going from standalone to interconnected SHS must be explored and quantified. Moreover, suitable energy sharing mechanisms need to be identified. These efforts are currently underway.

Table 4
Optimal SHS sizes that satisfy the different LLP criteria, along with the required converter sizes and the performance of these system sizes on the system metrics.

LLP [–]	Tier	PV (Wp)	Battery [Wh]	Converter [W]			Lifetime	R_{dump}	LLP
				PV	Load	Battery	[Years]	[–]	[–]
≤0.1	1	20	60	15	12	15	6.2	0.82	0.047
	2	70	210	53	51	52	5.9	0.48	0.1
	3	380	720	285	154	259	5.8	0.81	0.1
	4	1620	2520	1215	1670	1660	5.4	0.89	0.099
	5	4050	5300	3038	3081	2961	5.7	0.99	0.089
≤0.05	1	20	60	15	12	15	6.2	0.82	0.047
	2	80	240	60	51	59	6.3	0.65	0.039
	3	340	860	255	154	229	6.0	0.56	0.042
	4	1500	2880	1125	1670	1661	5.7	0.73	0.046
	5	3800	6150	2850	3081	2777	6.1	0.84	0.0431
≤0.02	1	20	70	15	12	15	6.8	0.80	0.019
	2	90	290	68	51	67	7.5	0.85	0.019
	3	420	1020	315	154	288	6.7	0.92	0.012
	4	1740	3560	1305	1670	1660	7	1.0	0.017
	5	4000	6600	3000	3081	2924	6.45	0.93	0.029

5. Conclusion

This study detailed an extensive methodology for the optimal sizing of SHS for every tier of the multi-tier framework for household electricity access. The genetic algorithm-based multi-objective optimization performed gave insights on the delicate interdependencies of the various system metrics on the SHS sizing. Moreover, meeting the energy demand of higher tiers, especially tier 5 is shown to be untenable with purely standalone SHS. Optimal system sizes for each tier of the MTF are presented, and the implications of these system sizes are discussed from the perspective of state-of-the-art SHS. Finally, an SHS interconnection-based microgrid is proposed as a potential means to climb up the so-called electrification ladder, especially to easily enable tier 4 and tier 5 levels of electricity access. The work presented in this paper is expected to shed light on the complex, multi-dimensional issue of electrification from the point of view of technical system design while exploring the intricate interdependencies of SHS parameters.

References

[1] IEA. Energy access Outlook 2017 – from poverty to prosperity. 1st ed. Organization for Economic Cooperation and Development, International Energy Agency; 2017.

[2] Global Off-Grid Lighting Association, Global off-grid solar market report – semi-annual sales and impact data, Tech. rep., GOGLA, Lighting Global and Berenschot; 2018.

[3] Heeten TD, Narayan N, Diehl JC, Verschelling J, Silvester S, Popovic-Gerber J, et al. Understanding the present and the future electricity needs: Consequences for design of future solar home systems for off-grid rural electrification. 2017 International conference on the Domestic Use of Energy (DUE) 2017. p. 8–15. https://doi.org/10.23919/DUE.2017.7931816.

[4] Bhatia M, Angelou N. Beyond connection, energy access redefined, The World Bank; 2015. <https://openknowledge.worldbank.org/bitstream/handle/10986/24368/Beyond0connect0d000technical0report.pdf?sequence=1&isAllowed=y>.

[5] Narayan N, Papakosta T, Vega-Garita V, Qin Z, Popovic-Gerber J, Bauer P, et al. Estimating battery lifetimes in solar home system design using a practical modelling methodology. Appl Energy 2018;228:1629–39. https://doi.org/10.1016/j.apenergy.2018.06.152<http://www.sciencedirect.com/science/article/pii/S0306261918310225>.

[6] Narayan N, Papakosta T, Vega-Garita V, Popovic-Gerber J, Bauer P, Zeman M. A simple methodology for estimating battery lifetimes in solar home system design. 2017 IEEE AFRICON 2017. p. 1195–201. https://doi.org/10.1109/AFRCON.2017.8095652.

[7] Vega-Garita V, Lucia DD, Narayan N, Ramirez-Elizondo L, Bauer P. Pv-battery integrated module as a solution for off-grid applications in the developing world.

[8] Narayan N, Vega-Garita V, Qin Z, Popovic-Gerber J, Bauer P, Zeman M. A modeling methodology to evaluate the impact of temperature on solar home systems for rural electrification. 2018 IEEE international Energy Conference (ENERGYCON) 2018. p. 1–6. https://doi.org/10.1109/ENERGYCON.2018.8398756.

[9] Narayan N, Qin Z, Popovic J, Bauer P, Zeman M. Evaluating the techno-economic feasibility of battery technologies in the context of solar home systems. 2018 20th European Conference on Power Electronics and Applications (EPE'18 ECCE Europe). 2018. p. P.1–.10.

[10] Ekren O, Ekren BY. Size optimization of a pv/wind hybrid energy conversion system with battery storage using response surface methodology. Appl Energy 2008;85(11):1086–101. https://doi.org/10.1016/j.apenergy.2008.02.016<http://www.sciencedirect.com/science/article/pii/S0306261908000524>.

[11] Hosseinalizadeh R, G HS, Amalnick MS, Taghipour P. Economic sizing of a hybrid (pv–wt–fc) renewable energy system (hres) for stand-alone usages by an optimization-simulation model: case study of Iran. Renew Sustain Energy Rev 2016;54:139–50. https://doi.org/10.1016/j.rser.2015.09.046<http://www.sciencedirect.com/science/article/pii/S1364032115010163>.

[12] Benavente-Araoz F, Lundblad A, Campana PE, Zhang Y, Cabrera S, Lindbergh G. Loss-of-load probability analysis for optimization of small off-grid pv-battery systems in bolivia. Energy Procedia 2017;142:3715–20. https://doi.org/10.1016/j.egypro.2017.12.266. proceedings of the 9th International Conference on Applied Energy. <http://www.sciencedirect.com/science/article/pii/S1876610217360009>.

[13] Chalise S, Sternhagen J, Hansen TM, Tonkoski R. Energy management of remote microgrids considering battery lifetime. Electric J 2016;29(6):1–10. https://doi.org/10.1016/j.tej.2016.07.003<http://www.sciencedirect.com/science/article/pii/S1040619016300987>.

[14] Bortolini M, Gamberi M, Graziani A, Pilati F. Economic and environmental bi-objective design of an off-grid photovoltaic–battery–diesel generator hybrid energy system. Energy Convers Manage 2015;106:1024–38. https://doi.org/10.1016/j.enconman.2015.10.051<http://www.sciencedirect.com/science/article/pii/S0196890415009735>.

[15] Smets A, Jäger K, Isabella O, Van Swaaij R, Zeman M. Solar energy - the physics and engineering of photovoltaic conversion, technologies and systems; 2016.

[16] Kougias I, Szabó S, Monforti-Ferrario F, Huld T, Bódis K. A methodology for optimization of the complementarity between small-hydropower plants and solar pv systems. Renewable Energy 2016;87:1023–30. https://doi.org/10.1016/j.renene.2015.09.073. optimization Methods in Renewable Energy Systems Design. <http://www.sciencedirect.com/science/article/pii/S0960148115303529>.

[17] Kellogg WD, Nehrir MH, Venkataramanan G, Gerez V. Generation unit sizing and cost analysis for stand-alone wind, photovoltaic, and hybrid wind/pv systems. IEEE Trans Energy Convers 1998;13(1):70–5. https://doi.org/10.1109/60.658206.

[18] Ayop R, Isa NM, Tan CW. Components sizing of photovoltaic stand-alone system based on loss of power supply probability. Renew Sustain Energy Rev 2018;81:2731–43. https://doi.org/10.1016/j.rser.2017.06.079<http://www.sciencedirect.com/science/article/pii/S1364032117310201>.

[19] Khatib T, Mohamed A, Sopian K. A review of photovoltaic systems size optimization techniques. Renew Sustain Energy Rev 2013;22:454–65. https://doi.org/10.1016/j.rser.2012.02.023<http://www.sciencedirect.com/science/article/pii/S1364032113001251>.

[20] Al-Falahi MD, Jayasinghe SDG, Enshaei H. A review on recent size optimization methodologies for standalone solar and wind hybrid renewable energy system. Energ Convers Manage 2017;143:252–74.

[21] De Schepper E, Lizin S, Durlinger B, Azadi H, Van Passel S. Economic and environmental performances of small-scale rural pv solar projects under the clean development mechanism: the case of cambodia. Energies 2015;8(9):9892–914.

[22] Paulitschke M, Bocklisch T, Böttiger M. Sizing algorithm for a pv-battery-h2-hybrid system employing particle swarm optimization. Energy Procedia 2015;73:154–62.

[23] Bhuiyan FA, Yazdani A, Primak SL. Optimal sizing approach for islanded micro-grids. IET Renew Power Gener 2015;9(2):166–75. https://doi.org/10.1049/iet-rpg.2013.0416.

[24] Meteotest, (software) meteonorm ver 7.1; 2014.

[25] Narayan N, Qin Z, Popovic-Gerber J, Diehl J-C, Bauer P, Zeman M. Stochastic load profile construction for the multi-tier framework for household electricity access using off-grid dc appliances. Energy Eff. doi:https://doi.org/10.1007/s12053-018-9725-6.

[26] Narayan NN. Electrical power consumption load profiles for households with dc appliances related to multi-tier framework of household electricity access; 2018.

doi:https://doi.org/10.4121/uuid:c8efa325-87fe-4125-961e-9f2684cd2086.

[27] Installation, commissioning and operating instructions for valve-regulated sta-tionary lead-acid batteries – solar battery data sheet; 2015.

[28] Camps X, Velasco G, de la Hoz J, Martín H. Contribution to the pv-to-inverter sizing ratio determination using a custom flexible experimental setup. Appl Energy 2015;149:35–45. https://doi.org/10.1016/j.apenergy.2015.03.050<http://www.sciencedirect.com/science/article/pii/S0306261915003347>.

[29] Islam S, Woyte A, Belmans R, Nijs J. Undersizing inverters for grid connection-What is the optimum?. In Proceedings of PV in Europe (pp. 780-783); 2002.

[30] MATLAB, gamultiobj Algorithm, The MathWorks Inc., Natick, Massachusetts; 2018.

[31] Kalyanmoy D. Multi objective optimization using evolutionary algorithms. John Wiley and Sons; 2001.